Bioaccumulation and toxicity of gold nanoparticles after repeated administration in mice

C. Lasagna-Reeves [a], D. Gonzalez-Romero [a,c], M.A. Barria [a,c], I. Olmedo [c,d], A. Clos [a], V.M. Sadagopa Ramanujam [b], A. Urayama [a,c], L. Vergara [a], M.J. Kogan [d,*], C. Soto [a,c,*]

[a] Department of Neurology, University of Texas Medical Branch, Galveston, TX, USA
[b] Department of Preventative Medicine, University of Texas Medical Branch, Galveston, TX, USA
[c] Mitchell Center for Alzheimer's Disease and Related Brain Disorders, Department of Neurology, University of Texas Medical School at Houston, Houston, TX 77030, USA
[d] Departamento de Química Farmacológica y Toxicológica, Facultad de Ciencias Químicas y Farmacéuticas, Universidad de Chile, Santiago, Chile and Centro para la investigación interdisciplinaria avanzada en ciencias de los materiales (CIMAT), Santiago, Chile

ARTICLE INFO

ABSTRACT

Gold nanoparticles (GNPs) offer a great promise in biomedicine. Currently, there is no data available regarding the accumulation of nanoparticles in vivo after repeated administration. The purpose of the present study was to evaluate the bioaccumulation and toxic effects of different doses (40, 200, and 400 µg/kg/day) of 12.5 nm GNPs upon intraperitoneal administration in mice every day for 8 days.

The gold levels in blood did not increase with the dose administered, whereas in all the organs examined there was a proportional increase on gold, indicating efficient tissue uptake. Although brain was the organ containing the lowest quantity of injected GNPs, our data suggest that GNPs are able to cross the blood–brain barrier and accumulate in the neural tissue. Importantly, no evidence of toxicity was observed in any of the diverse studies performed, including survival, behavior, animal weight, organ morphology, blood biochemistry and tissue histology. The results indicate that tissue accumulation pattern of GNPs depend on the doses administered and the accumulation of the particles does not produce subacute physiological damage.

Introduction

Nanoparticles (NPs) offer a great possibility for biomedical application, not only to deliver pharmaceutics, but also to be used as novel diagnostic and therapeutic approaches [1]. The small sizes of NPs imply that they could get close to a biological target of interest. Furthermore, metallic NPs can be made to resonantly respond to a time-varying magnetic field, with advantageous results related to the transfer of energy to the particles [2,3]. This leads to its use as a hyperthermic agent, thereby delivering toxic amounts of thermal energy to targeted bodies such as tumors [4–7].

Gold NPs (GNPs) shows several features that make them well suited for biomedical applications, including straightforward syn-thesis, stability, and the ability to selectively incorporate with recognition molecules such as peptides or proteins [2]. In a recent report, we demonstrated the feasibility of using targeted GNPs for the remote removal of Alzheimer's amyloid deposits by using local heat dissipated by irradiation of the particles with weak microwaves [5,8]. This type of approaches may be considered as a type of "molecular surgery" or "thermal scalpel" that has the potential to halt or slow the progression of the disease [3,9]. However, for the application of GNPs in therapy and drug delivery it is necessary to know the bioaccumulation and local or systemic toxicity associated to them. Also in the case of use in Central Nervous System (CNS), it is important to assess whether GNPs can cross the blood brain barrier to reach the neural tissue in meaningful quantities.

The particle size-dependent organ distribution of GNPs has been studied in vivo [10–14]. Hyllier and Albertch showed that orally administrated GNPs appeared in various tissues in mice and that the amount of absorption and distribution in the body inversely correlated with the size of the particles [10]. In most studies, systemically administrated NPs were primarily taken up by liver and spleen in a large quantity and small amounts distributed in the lung, kidney, heart, and brain after single administration. However, little is known about biodistribution, accumulation and toxicity of GNPs after repeated administration.

Materials and methods

Synthesis and characterization of GNPs

GNPs were synthesized according to Levy et al. [15] by citrate reduction of $HAuCl_4$. The colloidal GNPs solution was filtered through 0.45 μm *Millipore* syringe filters to remove any precipitate; the pH was adjusted to 7 using dilute NaOH solution, and the filtrate was stored at 4 °C. To determine the size, shape, and aggregation state, GNPs were observed by transmission electron microscopy (TEM) and UV–Visible Spectrophotometry, as previously described [16].

During the synthesis of GNPs a 1 nM solution was prepared. To obtain the desired doses, 10 mL of the 1 nM solution was centrifuged at 13,500 rpm for 10 min and the obtained pellet was resuspended in sodium citrate 1.2 mM to obtain the following concentrations: 1 nM (11 μg of gold/ml), 5 nM (55 μg of gold/ml) and 10 nM (110 μg of gold/ml). The solutions were a dark red color with a maximum of absorbance centered at 520 nm.

Animals and GNPs treatment

Male C57/BL6 mice of 12 weeks old were used for the experiments. The mice had free access to food and water, and were maintained on a 12 h dark/light cycle in a room with controlled temperature (25 ± 2 °C). Thirty-two mice were randomly divided into four groups: one control group and three experimental groups with different doses of GNPs. Mice received intraperitoneal (i.p.) injections of approximately 100 μL of GNPs solution (adjusting the final volume with the animal weight for the given dose) at doses of 40, 200, 400 μg/kg/day daily for 8 days. The doses used were chosen based on in vitro studies of GNPs toxicity in neuroblastoma cells in culture (data not shown) showing that GNPs did not produce significant toxicity up to 10 nM concentration, which correspond to the quantity on the highest dose. Control group was treated with vehicle solution (1.2 mM sodium citrate). The body weight of animals and their behavior were carefully recorded daily during the course of the experiment. One day after the last injection (day 9), mice were sacrificed, and the blood, liver, spleen, kidney, lungs, and brain were collected immediately. Serum from mouse blood was isolated by centrifugation at 3000 rpm for 10 min. A part of the organs was stripped and immediately fixed in a 10% formalin solution for further histopathological evaluation. The remaining samples were stored at −80 °C for the quantification of gold content in each tissue.

Analytical procedures for determination of gold in tissues

Digestion. Tissue samples were dried completely in a clean oven at 60–70 °C. Each dried tissue was digested to white ash using 30% hydrogen peroxide (GFS Chemical; Powell, OH) at 50–60 °C followed by digestion with concentrated ultra-pure trace-metal free nitric acid (0.1 mL, GFS Chemicals). The digested white ash was dissolved in 0.25 N nitric acid (1–4 mL, depending on the weight of the digested tissue). In order to increase the reliability of the gold measurements, two different analytical techniques were used, graphite furnace atomic absorption spectrophotometry (GF-AAS),[17,18] and inductively coupled plasma-mass spectrometry (ICP-MS) [12].

Graphite furnace atomic absorption spectrophotometry (GF-AAS). GF-AAS was performed using a Perkin–Elmer Model-5100 atomic absorption spectrophotometer equipped with a Perkin–Elmer HGA-600 graphite furnace with a Zeeman-5100 deuterium arc correction and a Perkin–Elmer-60 auto-sampler attached to graphite furnace. Pyrolytically coated graphite tubes with a L'vov platform

were used for all GF-AAS analysis. Each digested sample was further diluted suitably (1:2–1:50 v/v, depending on the tissue type and amount) using 0.25 N ultra-pure nitric acid prior to analysis. Elemental gold standard (Sigma Aldrich Chemical Co., Milwaukee, WI) was used for all calibration curves. All GF-AAS analyzes were performed at a temperature of 1800 °C.

Inductively coupled plasma-mass spectrometry (ICP-MS). A PlasmaQuad-3 ICP-MS instrument (V.G Elemental, Cheshire, UK) was used to quantify gold in the digested tissue samples. This instrument uses an 8000 °C temperature radio frequency-generated argon plasma to atomize and ionize gold ions to singly charged mass ions and the mass-to-charge (m/z) ratio signals were used to quantify the elements. Bismuth (209Bi) 1 ng/mL, was added to all samples as an internal standard in order to correct errors due to instrument drifts during data acquisitions. The digested samples were diluted suitably using 1% nitric acid, aspirated and then nebulized using a quartz Meinhard micro-concentric type nebulizer into the argon plasma via a peristaltic pump with a flow rate of approximately 0.9–1.0 mL/min. Mass spectral acquisitions were carried out using pulse-counting scanning mode with the following instrumental parameters: mass range scanned 190–220 m/z with 19 channels per mass, three points per peak, and 10.24 ms dwell time on each isotopic mass. The instrument control, methods procedures, and the data system, including calculations and statistics were operated via a personal computer with Plasma Vision Software. Nitric acid (1%) blanks were run in between samples to correct the background levels.

Estimation of the number of GNPs in the brain. To estimate the number of nanoparticles in the brain we used the following equation, as previously described [19].

$$C = Nt/Np.$$

where C is the concentration of nanoparticles in the brain (nanoparticles/per brain). Nt is the total number of gold atoms in the brain and Np is the number of atoms per nanoparticle of 12.5 nm (approximately 60,000 according to Liu et al. [19]). Nt was experimentally measured by ICP-MS or GF-AAS considering the brain weight and subtracting the gold level in control samples.

Toxicological studies

General examination. After administration of GNPs, animals were examined daily for survival and evident behavioral or motor impairments. Mice were also weighed every day. To examine morphological changes, the brain, lungs, liver, spleen, heart, and kidneys were removed and weighed.

Serum biochemical analysis. Whole blood was centrifuged twice at 3000 rpm for 10 min in order to separate serum. Using a biochemical autoanalyzer (Type 7170, Hitachi), serum biochemical analysis was carried out to determine the serum level of total bilirubin (TBIL) and alkaline phosphatase (ALKP) to evaluate liver function. Nephrotoxicity was assessed by determination of the levels of uric acid (URIC), urea nitrogen (UREA), and creatinine (CREA).

Hematological analysis. An hematological autoanalyzer (Coulter T540 hematology system, Fullerton) was used to determine hematological parameters such as red blood cells (RBC), white blood cells (WBC), hemoglobin, hematocrit, mean corpuscular volume, mean corpuscular hemoglobin, mean corpuscular hemoglobin concentration, red blood cell distribution width, neutrophils, lymphocytes, monocytes, eosinophils, basophils, and platelets.

Histopathological examination. Tissues fixed with 10% formalin were embedded in paraffin blocks, and then sliced into 5 μm in thickness. Hematoxylin-eosin staining was performed as described [20]. The bright-field images were acquired using a Nikon Eclipse 800 microscope equipped with a Nikon DXM1200 color CCD camera (Nikon Instruments Inc., Melville, NY).

Statistical analysis. Data was compared by one-way analysis of variance (ANOVA) followed by Bonferroni's multiple comparison test using the Prism 4.0 program (GraphPad Software, Inc., La Jolla, USA). The criterion for statistical significance was $p < 0.05$.

Results

GNPs synthesis and characterization

GNPs of 12.5 ± 1.7 nm were synthesized by reduction of $HAuCl_4$ with sodium citrate according with the procedure described by Levy et al. [15]. It is well known that GNPs exhibit the localized surface plasmon resonance phenomenon, which is manifested by an absorption band in the visible region of the optical spectrum. The GNPs synthesized showed a defined plasmon resonance peak at 520 nm (Fig. 1A), which was attributed to the presence of 12–13 nm citrate GNPs. The absence of absorbance at wavelengths greater than 600 nm indicated their well dispersed state in solution [21]. GNPs were further analyzed by TEM analysis of the colloidal gold solution. TEM image of GNPs (Fig. 1B) showed particles of small sizes (12.5 ± 1.7 nm) with regular shapes and narrow size distribution. Quantitative analysis of NPs size was performed by measuring the core diameter of 200 individual particles from multiple micrographs (Fig. 1B, inset).

Tissue distribution of GNP after repeated administration

To determine the distribution of GNPs in tissues, we employed two different methods to measure gold in various tissues, including brain, liver, kidney, spleen, and lungs. With both ICP-MS and GF-AAS, the amounts of gold detected in each tissue were similar. After GNP i.p. injection at the doses of 40, 200, and 400 μg/kg/day for 8 days and subsequent withdrawal for 1 day, we found significant increase of the gold levels in blood and organs examined (Fig. 2), suggesting that i.p. administrated GNPs were absorbed into systemic circulation and distributed into tissues. To rule out that particles remained in the peritoneal cavity, we have done studies to analyze the bioavailability after i.p. injection. The data showed a relatively slow absorption of GNPs from the peritoneal cavity to the blood, but our estimation is that virtually 100% of the material administered reached the blood (data not shown). The quantity in blood remained at similar levels between 0.019 and 0.027 ng/μL, regardless of the doses administered. Indeed, the blood levels of gold were not statistically significantly different after 8 days of administration of 40, 200 and 400 μg/kg/day of GNPs (Fig. 2).

Then, we examined the bioaccumulation of GNPs in brain, liver, kidney, spleen, and lung. In the brain, there was significant and progressive accumulation of gold in a dose-dependent manner, reaching quantities much higher than the reported physiological levels in brain [22]. Considering the relatively constant levels of gold in blood after GNPs administration at different doses, the increased accumulation of gold in the brain suggest non-saturable uptake of GNPs from the blood to the brain. These observations are supported by a previous study suggesting that GNPs may be able to cross the blood–brain barrier [10]. The average number of GNPs in the brain was 53,466, 71,419, and 166,352 for animals treated with 40, 200, and 400 μg/kg/day, respectively (Supplementary Table 1).

In kidney, liver, spleen, and lungs, there was significant increase in the amount of gold after repeated injection of GNPs (Fig. 2). The bioaccumulation profile of gold/g of tissue showed that spleen > liver = kidney > lungs > brain. However, considering the different sizes of the organs, the total% of injected dose obtained in the entire organ was highest in liver, followed by kidney and spleen (Table 1). Interestingly the percentage of gold accumulated decreases when the GNPs dose increases, suggesting efficient clearance of GNPs from the body.

Toxicological studies

We tested if GNPs treatment produces sub-acute toxicity in mice during the course of the study. We observed no mortality or any gross behavioral changes in mice receiving GNPs at the doses studied. There was no effect either of GNPs treatment on the body weight (Supplementary Fig. 1A). Tissue size, color, and morphologies also remain unchanged after treatment with GNPs (Supplementary Fig. 1B). No evidences of atrophy, congestion, or inflammation were observed.

To further search for abnormalities, the weight coefficient of each organ to body was calculated. No significant differences were observed for any of the organs studied as compared with controls untreated animals (Table 2). These observations indicate that extensive inflammation might not be induced in the mice after administration of gold nanoparticles, which is confirmed by the macroscopic morphological examination described later.
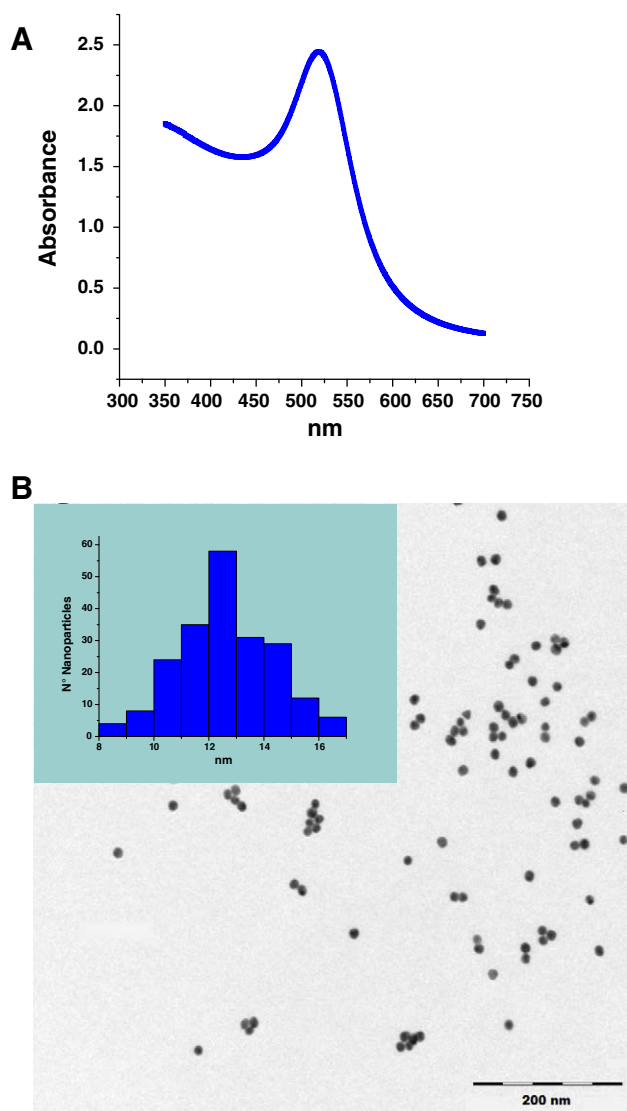

Fig. 1. Characterization of gold nanoparticles. GNPs were synthesized following the procedure described by Levy et al. [15]. (A) UV–Vis spectra of 5 nM GNPs and (B) transmission electron microscopic analysis of the particle morphology and size. The inset shows the distribution diameter of the GNPs obtained.
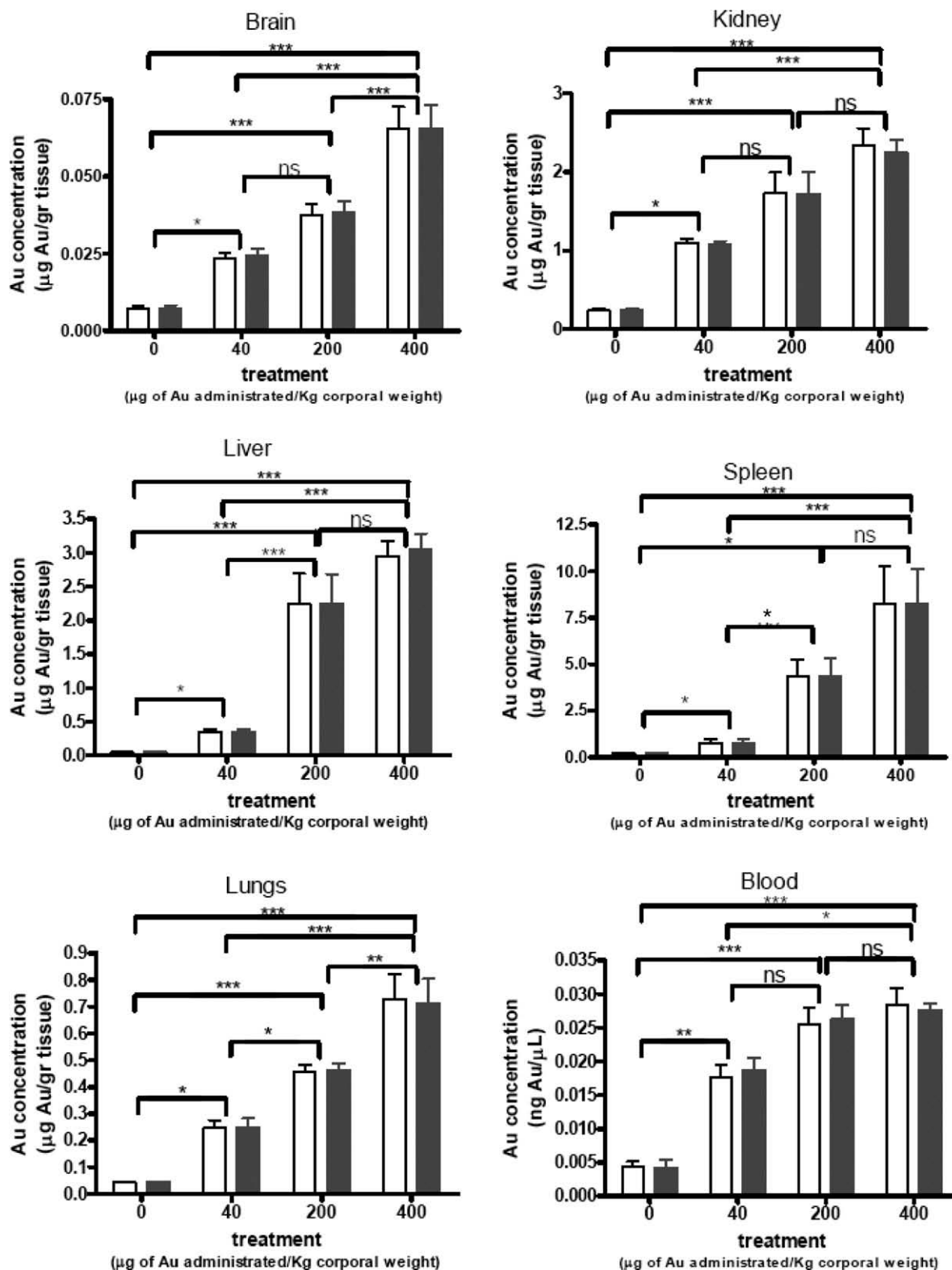
Fig. 2. Gold accumulation in body tissues. Animals were injected i.p. with various concentrations of GNPs (40, 200, and 400 μg/kg) for 8 consecutive days. After 1 day of withdrawal following the last injection, animals were sacrificed and blood and organs were extracted and analyzed by GF-AAS (white bar) and ICP-MS (black bar) to measure accumulated gold. The values correspond to the gold concentration relative to the weight of the dry tissue. Bars represent mean ± standard error; data were analyzed by ANOVA with Bonferroni's post test; ns: no significant difference, $^*p < 0.05$, $^{**}p < 0.01$, and $^{***}p < 0.001$.

To determine if GNPs produce renal toxicity, we determined the levels of urea nitrogen and creatinine in blood, which are metabolites associated with the functionality of the kidney. The levels of total bilirubin and alkaline phosphatase in blood were tested as a measure of hepatic and biliary functionality. In addition, we determined the levels of uric acid, since hypouricemia (decrease of uric acid in the blood) is a common sign of drug toxicity. A detailed analysis of all these metabolites in serum of animals treated with

Table 1
Bioaccumulation of GNPs with respect to the total injected dose in different organs (% ID/organ).

µg/kg/day	ICP-MS			GF-AAS		
	40	200	400	40	200	400
Brain	0.023 ± 0.006	0.006 ± 0.001	0.006 ± 0.001	0.022 ± 0.006	0.006 ± 0.001	0.006 ± 0.001
Lung	0.037 ± 0.013	0.011 ± 0.001	0.006 ± 0.002	0.036 ± 0.013	0.011 ± 0.001	0.006 ± 0.002
Spleen	0.204 ± 0.199	0.291 ± 0.219	0.096 ± 0.034	0.206 ± 0.198	0.281 ± 0.203	0.096 ± 0.034
Kidney	0.398 ± 0.173	0.184 ± 0.046	0.139 ± 0.058	0.413 ± 0.176	0.186 ± 0.044	0.139 ± 0.056
Liver	1.983 ± 0.566	1.828 ± 0.881	1.355 ± 0.361	2.009 ± 0.587	1.812 ± 0.867	1.320 ± 0.357

Table 2
Weight coefficient of liver, spleen, kidney, lung, and brain after exposure to nanoparticles.

Groups	Body weight (g) after treatment	Liver (mg/g)	Spleen (mg/g)	Kidney (mg/g)	Lung (mg/g)	Brain (mg/g)
Control	26.7 ± 1.1	53.3 ± 3.7	2.6 ± 0.2	7.9 ± 0.6	1.7 ± 0.2	16.9 ± 0.7
40 µg/kg/day	28.3 ± 1.0	54.8 ± 3.8	2.4 ± 0.3	7.4 ± 0.4	1.7 ± 0.3	16.9 ± 0.8
200 µg/kg/day	26.4 ± 1.9	54.1 ± 6.9	2.6 ± 0.7	7.8 ± 0.8	1.7 ± 0.3	17.2 ± 0.7
400 µg/kg/day	27.7 ± 1.6	56.4 ± 3.9	2.9 ± 0.3	7.5 ± 0.6	1.8 ± 0.5	16.7 ± 0.8

Data was analyzed by One-way ANOVA followed by Bonferroni's multiple comparison test and the differences between the distinct doses and control for each organ were not significant.

different doses of GNPs as compared to controls showed no statistically significant differences in any of the parameters tested (Table 3). Additional hematological studies were done to assess changes on the levels of red blood cells, white blood cells, hemoglobin, hematocrit, mean corpuscular volume, mean corpuscular hemoglobin concentration, red blood cell distribution width, neutrophils, lymphocytes, monocytes, eosinophils, basophils, and platelets. None of these parameters showed any statistical difference between the control and the experimental mice groups (data not shown).

Finally, in order to search in more detail for possible toxic effects, histological examination of various tissues was done. Mice exposed to GNPs showed no tissue damage in any of the sections obtained from the kidney, liver, spleen, brain or lungs (Fig. 3).

Discussion

Nanotechnology has recently emerged as a promising approach for treatment and diagnosis of a variety of diseases [1]. Due to the far-ranging claims that have been made about potential applications of nanotechnology, it is important to assess carefully the potential for these molecules to accumulate in the body and produce undesired side effects. GNPs are particularly promising for their easy synthesis in various shapes and the ability to conjugate them with peptides and proteins to target them to interact with specific molecules [3]. In addition, GNPs experience plasmon resonance with light [2]. This is a process whereby the electrons of the gold resonate in response to incoming radiation causing them to both absorb and scatter light. This effect can be harnessed to either destroy tissue by local heating or to release molecules of therapeutic importance.

In order to use GNPs in drug delivery, diagnosis, and treatment, it is essential to characterize the bioaccumulation and toxicity associated to repeated administration of these molecules. In this study, we evaluated the bioaccumulation and sub-acute toxicity of GNPs after administration of size-sorted GNPs at three different doses for 8 days into wild type mice. After repeated injection, the gold concentration in biological samples was determined by GF-AAS and ICP-MS and the measures resulted in similar and reproducible values. The levels of gold in blood and tissues in control group showed the expected physiological concentrations of gold in each sample. In all organs studied, there was a significant increase in gold levels after treatment, which was proportional to the dose administered. However, the levels of gold in blood did not increase in proportion to the dose, indicating that GNPs are mostly uptaken and accumulated by tissues. In order to assess tissue uptake, as much blood as possible was collected from the mice to maximize removal of residual blood from the organs. The residual amount of blood present in the organs is not known. However, even assuming that no blood was removed from the organs, our estimation is that from the quantity obtained in tissues, the contribution of blood is less than 6%, 2%, 3%, 1%, and 7.5% for the values we report in brain, kidney, liver, spleen, and lung, respectively. These values were calculated by the experimentally measured quantities of GNPs in blood and the known values of the vascular space in each tissue in mice. Therefore, we conclude that the GNPs measured in the tissues have a very small contribution from the blood in the tissue. A previous study by Cho et al. demonstrated that after administration of a single dose of 13 nm GNPs injected intravenously, it is possible to find gold in various organs 24 h and 7 days after injection [23]. Their conclusion is that the organ gold concentration is dependent on the time after injection. In

Table 3
Biochemical parameters in the serum of mice treated with GNPs.

Groups	URIC (mg/dL)	CREA (mg/dL)	UREA (mg/dL)	TBIL (mg/dL)	ALKP (U/L)
Control	3.45 ± 0.8	0.24 ± 0.08	26.25 ± 2.06	1.25 ± 0.53	89.25 ± 9.8
40 µg/kg/day	3.93 ± 0.6	0.27 ± 0.02	24.01 ± 2.44	0.90 ± 0.28	86.60 ± 10.9
200 µg/kg/day	4.02 ± 1.1	0.26 ± 0.06	24.02 ± 3.65	0.75 ± 0.31	91.01 ± 16.4
400 µg/kg/day	4.17 ± 0.8	0.24 ± 0.05	26.20 ± 2.58	0.52 ± 0.26	76.66 ± 3.7

Data was analyzed by One-way ANOVA followed by Bonferroni's multiple comparison test and the differences between the distinct doses and control for each parameter were not significant.
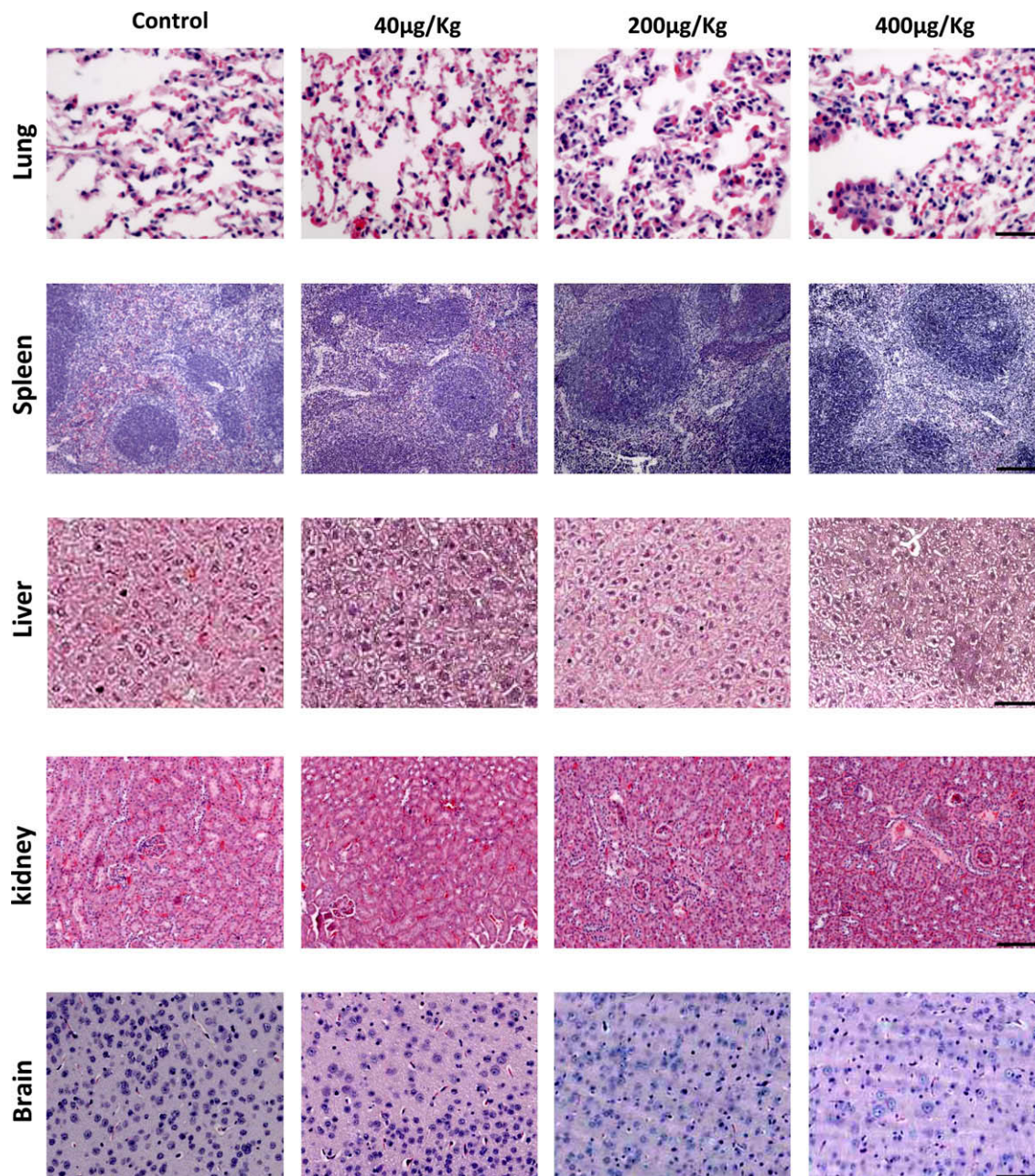
Fig. 3. Histological analysis of various organs after GNPs treatment. Tissues were stained with hematoxilin/eosin as indicated in Materials to assess for potential effects of GNPs treatment on the organ morphology and cellular damage. The size of the bar corresponds to the following: lung, 130 μm; spleen, 35 μm; liver, 30 μm; kidney, 100 μm; brain 75 μm.

our repeated dose study, in which the time was fixed and the dose was varied, we found that gold accumulation is dependent on the dose administered.

Particularly interesting is the case of brain; considering the relatively constant levels of gold in blood after GNPs administration at different doses, the increased accumulation of gold in the brain suggest non-saturable uptake of GNPs across the blood–brain barrier. Although we can rule out that a significant amount of the GNPs measured in brain is in the blood, we cannot completely discard that the particles might associate to vessel walls in brain capillaries. However, preliminary experiments in which fluorescently labeled GNPs were injected i.p. into animals showed that we can retrieve particles in the brain parenchyma (data not shown). Our findings showing a clear increase on GNPs accumulation at increas-

ing doses support the possibility to use nanoparticles to target the brain without producing detectable toxicity. This is important for the utilization of GNPs for potential treatment and diagnosis of neurodegenerative disorders.

The accumulation of 12.5 nm GNPs in kidney could be explained by the bigger size of the particle with respect to the glomerular pores that measure 5.5 nm. So it is unlikely that NPs can pass through the glomerular filtration due to its size and negative electrostatic potential [24]. In the spleen and liver, the bioaccumulation of GNPs may be regulated by the reticulo-endothelial system, which is part of the immune system involved in the uptake and metabolism of exogenous molecules and particles in these tissues. In addition, it is also known that NPs are taken up by kupffer cells in the liver and by macrophages in other places, regardless of

the particle size [25]. Semmler-Behnke et al. observed that a considerable percentage of GNPs of 18 nm are removed from the blood and trapped predominantly in the liver and spleen [13]. A small amount of the injected intravenous dose was excreted via the hepatobiliary system into the feces, but renal excretion was extremely low.

The pharmacokinetic, bioavailability, bioaccumulation, clearance and toxicity of NPs are likely dependent of the particle composition, size and surface characteristics. These properties may be altered to reach the most appropriate balance for different applications. One factor regulating the pharmacological properties of NPs may be the electrostatic state of the particle. The surface of GNPs has negative charge due to citrates absorbed during its production. The 12.5 nm GNPs used in this study have a zeta potential of −53 mV as described by Olmedo et al. [8].

Accumulation of GNPs in different organs after repeated administration did not produce any mortality or any indication of toxicity as assessed by animal behavior, tissue morphology, serum biochemistry, hematological analysis, and histopathological examination.

Acknowledgments

Appendix A. Supplementary material

Supplementary material associated with this article can be found, in the online version, at doi:10.1016/j.bbrc.2010.02.046.

References

[1] S.D. Caruthers, S.A. Wickline, G.M. Lanza, Nanotechnological applications in medicine, Curr. Opin. Biotechnol. 18 (2007) 26–30.
[2] D. Pissuwan, S.M. Valenzuela, M.B. Cortie, Therapeutic possibilities of plasmonically heated gold nanoparticles, Trends Biotechnol. 24 (2006) 62–67.
[3] M.J. Kogan, I. Olmedo, L. Hosta, A.R. Guerrero, L.J. Cruz, F. Albericio, Peptides and metallic nanoparticles for biomedical applications, Nanomedicine 2 (2007) 287–306.
[4] I.H. El-Sayed, X. Huang, M.A. El-Sayed, Selective laser photo-thermal therapy of epithelial carcinoma using anti-EGFR antibody conjugated gold nanoparticles, Cancer Lett. 239 (2006) 129–135.
[5] M.J. Kogan, N.G. Bastus, R. Amigo, D. Grillo-Bosch, E. Araya, A. Turiel, A. Labarta, E. Giralt, V.F. Puntes, Nanoparticle-mediated local and remote manipulation of protein aggregation, Nano. Lett. 6 (2006) 110–115.
[6] V.P. Zharov, K.E. Mercer, E.N. Galitovskaya, M.S. Smeltzer, Photothermal nanotherapeutics and nanodiagnostics for selective killing of bacteria targeted with gold nanoparticles, Biophys. J. 90 (2006) 619–627.
[7] L.R. Hirsch, R.J. Stafford, J.A. Bankson, S.R. Sershen, B. Rivera, R.E. Price, J.D. Hazle, N.J. Halas, J.L. West, Nanoshell-mediated near-infrared thermal therapy of tumors under magnetic resonance guidance, Proc. Natl. Acad. Sci. USA 100 (2003) 13549–13554.
[8] I. Olmedo, E. Araya, F. Sanz, E. Medina, J. Arbiol, P. Toledo, A. varez-Lueje, E. Giralt, M.J. Kogan, How changes in the sequence of the peptide CLPFFD-NH2 can modify the conjugation and stability of gold nanoparticles and their affinity for beta-amyloid fibrils, Bioconjug. Chem. 19 (2008) 1154–1163.
[9] M. Everts, Thermal scalpel to target cancer, Expert. Rev. Med. Devices 4 (2007) 131–136.
[10] J.F. Hillyer, R.M. Albrecht, Gastrointestinal persorption and tissue distribution of differently sized colloidal gold nanoparticles, J. Pharm. Sci. 90 (2001) 1927–1936.
[11] G. Sonavane, K. Tomoda, K. Makino, Biodistribution of colloidal gold nanoparticles after intravenous administration: effect of particle size, Colloids Surf. B Biointerfaces 66 (2008) 274–280.
[12] W.H. De Jong, W.I. Hagens, P. Krystek, M.C. Burger, A.J. Sips, R.E. Geertsma, Particle size-dependent organ distribution of gold nanoparticles after intravenous administration, Biomaterials 29 (2008) 1912–1919.
[13] M. Semmler-Behnke, W.G. Kreyling, J. Lipka, S. Fertsch, A. Wenk, S. Takenaka, G. Schmid, W. Brandau, Biodistribution of 1.4- and 18-nm gold particles in rats, Small 4 (2008) 2108–2111.
[14] J.F. Hainfeld, D.N. Slatkin, T.M. Focella, H.M. Smilowitz, Gold nanoparticles: a new X-ray contrast agent, Brit. J. Radiol. 79 (2006) 248–253.
[15] R. Levy, N.T. Thanh, R.C. Doty, I. Hussain, R.J. Nichols, D.J. Schiffrin, M. Brust, D.G. Fernig, Rational and combinatorial design of peptide capping ligands for gold nanoparticles, J. Am. Chem. Soc. 126 (2004) 10076–10084.
[16] M.J. Kogan, N.G. Bastus, R. Amigo, D. Grillo-Bosch, E. Araya, A. Turiel, A. Labarta, E. Giralt, V.F. Puntes, Nanoparticle-mediated local and remote manipulation of protein aggregation, Nano Lett. 6 (2006) 110–115.
[17] D.F. Kehoe, D.M. Sullivan, R.L. Smith, Determination of gold in animal tissue by graphite furnace atomic absorption spectrophotometry, J. Assoc. Anal. Chem. 71 (1988) 1153–1155.
[18] V.M. Ramanujam, K. Yokoi, N.G. Egger, H.H. Dayal, N.W. Alcock, H.H. Sandstead, Polyatomics in zinc isotope ratio analysis of plasma samples by inductively coupled plasma-mass spectrometry and applicability of nonextracted samples for zinc kinetics, Biol. Trace Elem. Res. 68 (1999) 143–158.
[19] X. Liu, M. Atwater, J. Wang, Q. Huo, Extinction coefficient of gold nanoparticles with different sizes and different capping ligands, Colloids Surf. B Biointerfaces 58 (2007) 3–7.
[20] J. Castilla, P. Saá, C. Hetz, C. Soto, In vitro generation of infectious scrapie prions, Cell 121 (2005) 195–206.
[21] J.Y. Shim, V.K. Gupta, Reversible aggregation of gold nanoparticles induced by pH dependent conformational transitions of a self-assembled polypeptide, J. Colloid Interface Sci. 316 (2007) 977–983.
[22] K.G. Kjellin, Trace elements in the cerebrospinal fluid in neurological diseases, Clin. Toxicol. 18 (1981) 1237–1245.
[23] W.S. Cho, M. Cho, J. Jeong, M. Choi, H.Y. Cho, B.S. Han, S.H. Kim, H.O. Kim, Y.T. Lim, B.H. Chung, J. Jeong, Acute toxicity and pharmacokinetics of 13 nm-sized PEG-coated gold nanoparticles, Toxicol. Appl. Pharmacol. 236 (2009) 16–24.
[24] M. Longmire, P.L. Choyke, H. Kobayashi, Clearance properties of nano-sized particles and molecules as imaging agents: considerations and caveats, Nanomedicine 3 (2008) 703–717.
[25] E. Sadauskas, H. Wallin, M. Stoltenberg, U. Vogel, P. Doering, A. Larsen, G. Danscher, Kupffer cells are central in the removal of nanoparticles from the organism, Part Fibre. Toxicol. 4 (2007) 10.